

Vol. 04, No. 01, pp. 30-53, June 2011

REMOVAL OF METHYLENE BLUE FROM AQUEOUS SOLUTIONS USING YEMEN BENTONITE

Abdulrakib Abdulwahab Masad Al-Wahbi* and Hani Ahmed Qasim Dammag**
Hadramout University of Science and Technology, Al-Mukalla, Hadramout, Republic of Yemen.

*Corresponding authors Email: abdalwahby_73@yahoo.com,

**dr_hani.dammag@yahoo.com.

(Received:27/10/2010 ; Accepted:30/3/2011)

ABSTRACT - Removal of Methylene Blue (MB) from aqueous solutions using Yemen bentonite as low-cost adsorbent have been studied as a function of temperature, particle size and solution pH . The adsorption capacity increased with increasing temperature (15 to 45°C) and solution pH value (2 to 12) and decreasing particle size (500-710 to 80-125). The maximum adsorption capacity was 500.0 (mg.g⁻¹) at T = 25°C, dp = 250-355 μm and pH = 12. The experimental data were analyzed by Langmuir, Freundlich, Temkin and Redlich-Peterson isotherms, and found that the Redlich-Peterson isotherm best fit the experimental data over the whole concentration range with R² values lie between 0.9986 and 0.9999. Thermodynamic parameters such as standard Gibbs free energy (ΔG°), standard enthalpy (ΔH°), and standard entropy (ΔS°) were calculated. The thermodynamic parameters of MB/clay system indicated spontaneous and endothermic nature of the adsorption process. The results demonstrate that Yemen bentonite is effective in the removal of MB from aqueous solutions and can be used as alternative of high cost commercial adsorbents.

Keywords:- Adsorption; Methylene Blue; Yemen bentonite.

NOMENCLATURE

ARE average relative of errors (dimensionless)

a_L parameter of Langmuir isotherm (dm³.mg⁻¹)

a_{RP} parameter of Redlich-Peterson isotherm [(dm³.mg⁻¹)^{1/β}]

A_T Temkin isotherm constant (dm³.mg⁻¹)

B_T	Temkin isotherm constant (dimensionless)
C_e	equilibrium liquid-phase concentration ($\text{mg}\cdot\text{dm}^{-3}$)
C_0	initial liquid-phase concentration ($\text{mg}\cdot\text{dm}^{-3}$)
d_p	mean particle diameter (μm)
K_F	parameter of Freundlich isotherm ($\text{dm}^{-3}\cdot\text{g}^{-1}$) ⁿ
K_L	parameter of Langmuir isotherm ($\text{dm}^{-3}\cdot\text{g}^{-1}$)
K_{RP}	parameter of Redlich-Peterson isotherm ($\text{dm}^{-3}\cdot\text{g}^{-1}$)
m	adsorbent mass (g)
q_e	equilibrium solid-phase concentration ($\text{mg}\cdot\text{g}^{-1}$)
$q_{e,\text{exp}}$	experimental equilibrium solid-phase concentration ($\text{mg}\cdot\text{g}^{-1}$)
$q_{e,\text{cal}}$	calculated equilibrium solid-phase concentration ($\text{mg}\cdot\text{g}^{-1}$)
q_m	maximum solid-phase concentration ($\text{mg}\cdot\text{g}^{-1}$)
R^2	linear regression correlation coefficient (dimensionless)
r_{av}	average pore diameter (Å)
S_{BET}	surface area calculated by BET equation ($\text{cm}^2\cdot\text{g}^{-1}$)
T	absolute temperature (K)
V	volume of liquid in adsorber (dm^3)
V_{mic}	micropore volume ($\text{cm}^3\cdot\text{g}^{-1}$)
V_{mes}	mesopore volume ($\text{cm}^3\cdot\text{g}^{-1}$)
V_{mac}	macropore volume ($\text{cm}^3\cdot\text{g}^{-1}$)
ϵ_p	particle porosity (dimensionless)
ρ_p	particle density ($\text{g}\cdot\text{cm}^{-3}$)
ρ_s	solid density ($\text{g}\cdot\text{cm}^{-3}$)
λ_{max}	maximum wavelength (nm)

1. INTRODUCTION

Water pollution is increasingly becoming a major concern besides air and soil pollution. It is a major element of 21st century environmental pollution, it includes the accumulation of pollutants in oceans, lakes, rivers and streams, of physical, chemical and biological substances that are either directly harmful or result in secondary and long-range effects.

Many industries, such as textiles, pulp mills, leather, printing, food, and plastics, use dyes in order to colour their products and consume substantial volumes of water. The

presence of very small amounts of dyes in water (less than 1 ppm for some dyes) is highly visible and undesirable⁽¹⁻²⁾. As a result, they generate a considerable amount of coloured waste water. It is recognize that public perception of water quality is greatly influenced by the colour. Over 100,000 commercially available synthesis dyes exist and more than 7×10^5 tons per year are produced annually⁽³⁾.

Cationic Dyes are widely used for paper, modified nylons, silk, wood, modified polyesters and tannin-mordanted cotton. These water-soluble dyes dissociate into anions and coloured cations in solution. These dyes have amino groups or alkylamino groups and consequently have an overall positive charge⁽⁴⁾.

The most important cationic dye is Methylene Blue (MB). It dissociates in aqueous solution like electrolytes into MB cation and the chloride ion. Methylene blue is widely used for printing calico, dyeing, printing cotton and tannin and dyeing leather. It is also used as a stain and has a number of biological uses. Although it is low toxicity, it can cause various harmful effects. On inhalation, it can give rise to short periods of rapid or difficult breathing while ingestion through the mouth produces a burning sensation and may cause nausea, vomiting, diarrhea, and gastritis. Accidental large dose creates abdominal and chest pain, severe headache, profuse sweating, mental confusion, painful micturation, and methemoglobinemia⁽⁵⁾. Due to those previous effects of MB on the health and it's used for the adsorption characterization of porous adsorbent with a potential application in the removal of pollutants from aqueous solution⁽⁶⁾ it was selected as a model compound in this work.

Due to increasingly stringent restrictions on the organic content of industrial effluents, it is necessary to eliminate dyes from wastewater before it discharged.

During the past three decades, several physical, chemical and biological methods are used to removes dyes from effluents. Among the physical methods available of dye removal, adsorption is found to be the most effective treatment for the removal of colour from wastewater and gives the best results as it can be used to remove different types of colouring materials⁽⁷⁾. Adsorption has been found to be superior to other techniques for wastewater treatment in terms of initial cost, flexibility, simplicity of design, ease of operation, insensitivity to toxic pollutants and does not result in the formation of harmful substances⁽⁸⁾.

Most commercial adsorption systems currently use activated carbon as adsorbent to remove dyes in wastewater because of its excellent adsorption ability. It has a good capacity for the adsorption of organic molecules^{(3); (9-10)}. Although, the overlying cost of activated

carbon and its regeneration problems led researchers to produce and use low-cost, abundance, and not need to regeneration adsorbents.

Low-cost adsorbents, including raw agricultural solid wastes and waste materials from forest industries such as maize cob ⁽¹¹⁾, palm-fruit bunch particles ⁽¹²⁾, bagasse pith ⁽¹³⁾, sawdust ⁽¹⁴⁾, papaya seeds ⁽¹⁵⁾, hazelnut shell ⁽¹⁶⁾, and have been used successfully as alternative to high cost commercial activated carbon.

Clay materials have been increasingly paid attention because of their low cost, abundance in most continents of the world, high specific surface area, and chemical and mechanical stabilities. In addition, clay materials have shown good results as an adsorbent for the removal of various metals ⁽¹⁷⁾, surfactants ⁽¹⁸⁾, and basic and acid dyes ⁽¹⁹⁻²⁰⁾.

Up to our knowledge, no research has been conducted using Yemen Bentonite as adsorbent. Therefore, the main aim of this study is to investigate the suitability of Yemen Bentonite as low-cost adsorbent for the removal of MB from aqueous solutions.

2. MATERIAL AND METHODS

2.1. Materials

The natural bentonite used in this work was collected from Al-Rayan zone, Al-Mukalla City, Hadramout Governorate, Republic of Yemen. The adsorbent was washed, crushed and sieved through different standard sieves into the desired particle size and used without any pre-treatment. The resulting sample was dried at 105 °C and stored in sealed containers prior to use.

Methylene Blue [C.I. Basic Blue 9, C₁₆H₁₈N₃SCl, M.W.= 319.9 g.g-mol⁻¹, and λ_{max}: 665 nm] supplied by Merck company (Germany) was used as principal adsorbate without further purification.

2.2. Characterization of Natural Bentonite

Chemical composition of bentonite was obtained using XR-F Spectrometer, ARL 9800, Switzerland.

Solid density, particle density and porosity for natural clay were obtained using mercury Poresizer 9320, Micromertics, USA.

The surface physical properties such as specific surface area, pore size distribution and total pore volume were measured by nitrogen adsorption–desorption isotherms using a

multipurpose apparatus Nova 2000 analyzer, Quantachrome Instruments, Japan. A BET analysis ⁽²¹⁾ from the amount of N₂ gas adsorbed at various partial pressures was used to determine the surface area (S_{BET}), and a single condensation point (p/p₀ = 0.95) was used to find the total pore volume (V_T). The average pore radius (r_{av}) was calculated using total surface area and total pore volume (r_{av} = 2V_T/S_{BET}). The volumes of micropores, mesopores, and macropores were calculated from N₂ adsorption isotherm by applying the Barrett-Joyner-Hallenda (BJH) method ⁽²²⁾.

2.3. Method

Batch adsorption experiments were carried out using bottle-point method ⁽²³⁾. In this method stock solution of MB (1000 mg.dm⁻³) was prepared and was subsequently diluted to the required initial concentrations. Adsorption capacity of the clay towards MB was determined by contacting a constant mass (0.05 g) of clay with a fixed volume (50 ml) in sealed glass bottles of different initial concentrations of dye solution. The bottles were agitated in an isothermal water-bath shaker for 5 h until equilibrium was reached. At the end of the adsorption time, a known volume of the solution was removed and centrifuged for analysis of the supernatant.

Calibration curve for MB was prepared by recording the absorbance values for a range of known concentrations of dye solution and the maximum absorbance was determined (λ_{max} = 665 nm). The value of λ_{max} was used in all subsequent investigations using this dye.

The concentration of MB in aqueous solution was then determined at λ_{max} = 665 nm using double beam UV-visible spectrophotometer (Shimadzu, Model UV 1601, Japan).

The amount of MB adsorbed onto clay, q_e (mg.g⁻¹), was calculated by the following equation:

$$q_e = \frac{(C_0 - C_e) \times V}{m} \quad (1)$$

Where C₀ and C_e are the initial and equilibrium concentrations of dye solution (mg.dm⁻³), respectively. V is the total volume of the dye solution (dm³), and m is the mass of clay used (g).

3. RESULTS AND DISCUSSION

3.1. Characterization of Natural Bentonite

Chemical analysis indicates the following composition: SiO₂, 62.38%; Al₂O₃, 13.60%; Fe₂O₃, 7.05%; CaO, 3.75%; MgO, 3.11%; K₂O, 2.63%.

The N₂ adsorption-desorption isotherm obtained for natural bentonite is shown in Figure 1. As shown in the Figure, the desorption branch of this isotherm exhibited hysteresis and correspond to the Type IV isotherm. The existence of the hysteresis loop in the isotherm is due to the capillary condensation of N₂ gas occurring in the mesopores and therefore, the Type IV isotherm is considered as the characteristic feature of the mesoporous materials ⁽²⁴⁾.

The sharp rise near $P/P_0 = 0.4$ corresponds to condensation in the primary mesopores. The well defined hysteresis loop between the adsorption and desorption branches can be classified as type H4 according to the IUPAC classification ⁽²⁴⁾. Physical characteristics of the Yemen natural bentonite such as the values of BET surface area (S_{BET}), total pore volume (V_T), micropore volume (V_{mic}), mesopore volume (V_{mes}), macropore volume (V_{mac}), and average pore radius (r_{av}) are listed in Table 1.

It is obvious from Table 1 that Yemen bentonite has high specific surface area ($82.3 \text{ cm}^2 \cdot \text{g}^{-1}$) and total pore volume ($0.109 \text{ cm}^3 \cdot \text{g}^{-1}$).

Pore size distribution is one of the most important parameters for any porous adsorbent because the size of pores must be larger than the adsorbate molecule volume to allow it to enter inside the adsorbent particle pores. Figure 2 shows pore size distribution (PSD) of bentonite calculated from N₂ adsorption isotherm by applying the Barrett-Joyner-Hallenda (BJH) method using desorption branch of the isotherms ⁽²²⁾. As illustrated in Figure 2, pores between 1.4 and 2.9 nm were dominant. Their average pore size is 2.997 nm determined by (BJH) method, which was in the mesopore range (pore size, 2–50 nm).

3.2. Adsorption Isotherms

Determining the distribution of MB between natural bentonite and the liquid phase when the system is a state of equilibrium is important in establishing the capacity of the clay for MB. Preliminary experiments showed that such equilibrium was established within 180 min; however, all equilibrium experiments were allowed to run for 300 min.

Plotting the amount of MB adsorbed at equilibrium (q_e) against final concentration in the aqueous phase (C_e) at different temperatures, different particle size ranges and different solution pH values gave a characteristic H-shaped curve as shown in Figures 3 to 5.

According to the slope of the initial portion of the curve of MB onto clay, this isotherm may be classified as H-shape according to Giles classification ⁽²⁵⁾. In this type of isotherm, the initial portion provides information about the availability of the active sites to the adsorbate and the plateau signifies the monolayer formation. The initial curvature indicates that a large amount of dye is adsorbed at a lower concentration as more active sites of clay are available.

As the concentration increases, it becomes difficult for a dye molecule to find vacant sites, and so monolayer formation occurs.

This type of isotherm suggests a high affinity of the MB molecules for the active sites of the clay surface, and also that there is no competition from the solvent for adsorption sites (25).

3.2.1. Effect of Solution Temperature

Figure 3 present the adsorption isotherms of MB onto clay at different temperatures (15, 25, 35 and 45°C) at constant particle size range 250-350 μm and $\text{pH} = 6 \pm 0.2$ of MB solution. From this Figure, it can be seen that the experimental adsorption capacity of clay increased from 420.0 to 471.4 (mg.g^{-1}) with an increase in temperature of solution from 15 to 45°C.

The enhancement in the adsorption capacity may be due to increasing the rate of diffusion of the adsorbate molecules across the external boundary layer and in the internal pores of the adsorbent particle, owing to the decrease in the viscosity of the solution (26).

Senthilkumar and co-workers (27) suggested that the increase in adsorption capacity with increase in temperature might be due to the possibility of an increase in the porosity and in the total pore volume of the adsorbent, an increase of number of active sites for the adsorption as well as an increase in the mobility of the MB molecules.

Increase of the adsorption capacity of clay by raising temperature indicate a chemisorptions mechanism, with an increasing number of molecules acquiring sufficient energy to undergo chemical reaction with clay. This conclusion was confirmed by the change in standard enthalpy (ΔH°) during the adsorption processes. Standard enthalpy change (ΔH°) at different temperatures has been calculated using Van't Hoff equation and was found to be positive value (32.3 $\text{kJ.g}^{-1}\text{mol}^{-1}$). Similar results show that the adsorption process of MB is an endothermic in nature were obtained by different researchers (28-29).

3.2.2. Effect of Particle Size Range

Figure 4 shows that a decrease in clay particle size led to an increase in equilibrium adsorption capacity. The experimental equilibrium adsorption capacity of clay for MB increased from 419.4 (mg.g^{-1}) to 452.2 (mg.g^{-1}) with decreasing particle size range from 500-710 μm to 80-125 μm . This behavior can be attributed to the inability of the large dye molecules to penetrate into the internal pore structure of clay. Apparently, breaking up large particle diameter to form smaller ones probably serves to open some tiny, sealed pores in the

clay which become available for adsorption, thus slightly increasing the total specific surface area of a given mass ⁽³⁰⁾. Several investigations have shown similar observation for clay minerals and other adsorbents ⁽³¹⁻³²⁾.

3.2.3. Effect of Solution pH

Figure 5 shows the effect of dye solution pH on the experimental equilibrium adsorption capacity of natural bentonite for MB over a wide pH range of 2-12. As shown in the Figure, that strong dependence of experimental equilibrium capacity on the solution pH, which increased from 395.9 to 489.5 (mg.g⁻¹) with increasing solution pH from 2 to 12. The strong dependence of adsorption on pH could be attributed to the fact that the surface charge of clay was greatly affected by solution pH. When the solution pH is greater than the pHzpc that equal to 7.2 for natural bentonite studied in this work, the negative charged clay surface is favorable for the adsorption MB dye. It can be said that natural clay surface exhibited positive zeta potential values at the lower pH values from pH 7.2, and with the increasing of pH, the surface of clay becomes more negatively charged, thereby increasing electrostatic attractions between positively charged dye anions (MB⁺) and negatively charged adsorption sites and causing an increase in the equilibrium dye adsorption capacity. Similar results was reported by Özdemir and co-workers ⁽³³⁾.

3.3. Isotherm models

The adsorption equilibrium data obtained for the MB onto natural bentonite were fitted into four different isotherm models to determine the most suitable model to represent the adsorption process. The isotherms used are the Langmuir isotherm, the Freundlich, the Temkin isotherm, and the Redlich-Peterson isotherm.

In order to quantitatively compare the applicability of different models, the average relative error (ARE) was calculated using equation 2 ⁽³⁴⁾:

$$ARE = \frac{1}{N} \left[\sum_{i=1}^N \left| \frac{q_{e,cal} - q_{e,exp}}{q_{e,exp}} \right| \right] \quad (2)$$

Where N is the number of data points, $q_{e,exp}$ and $q_{e,cal}$ (mg.g⁻¹) are the experimental and the calculated values of the equilibrium adsorbate solid concentration in the solid phase, respectively. The values of ARE is used as measures of the fitting of the data to an isotherm equation, small values of ARE would indicate a perfect fit.

3.3.1. Langmuir isotherm

The Langmuir isotherm (1918)⁽³⁵⁾ is valid for monolayer adsorption on a homogenous adsorbent surface containing a finite number of identical site and no interaction between adsorbate molecules.

The Langmuir expression is represented by the following equation:

$$q_e = \frac{1 + K_L C_e}{1 + a_L C_e} \quad (3)$$

This may be converted into a linear form which is convenient for plotting and determining the constants K_L ($\text{dm}^3 \cdot \text{g}^{-1}$) and a_L ($\text{dm}^3 \cdot \text{mg}^{-1}$):

$$\frac{C_e}{q_e} = \frac{a_L}{K_L} C_e + \frac{1}{K_L} \quad (4)$$

The essential characteristics of the Langmuir isotherm can be expressed in terms of a dimensionless equilibrium parameter (R_L), which is defined by Hall et al., 1966⁽³⁶⁾:

$$R_L = \frac{1}{1 + a_L \cdot C_0} \quad (5)$$

Where R_L is a dimensionless constant separation factor, C_0 is the initial concentration of dye ($\text{mg} \cdot \text{dm}^{-3}$) and K_L is the Langmuir adsorption constant ($\text{dm}^3 \cdot \text{g}^{-1}$).

The value of R_L indicates the shape of the isotherms to be either unfavorable ($R_L > 1$), linear ($R_L = 1$), favorable ($0 < R_L < 1$) or irreversible ($R_L = 0$).

Linear plots of (C_e/q_e) versus (C_e) with high linear regression coefficient values ($R^2 > 0.999$) for the adsorption of MB onto clay at different temperatures, particle size ranges and solution pH values (Figures not shown) suggest the applicability of the Langmuir isotherm and demonstrate monolayer coverage of the adsorbate on the outer surface of the adsorbent⁽³⁷⁾.

The values of K_L and a_L have been calculated for the different variables studied using equation 4 and listed with the corresponding values of linear regression coefficient (R^2) and the average relative of the errors function (ARE) in Table 2. The values of the constant (K_L/a_L) correspond to the maximum adsorption capacity (q_m) of the clay for MB were also calculated and listed in Table 2.

It is clear from Table 2 that all variables play an interesting role in the adsorption of MB. Increasing temperature from 15°C to 45°C led to an increase in the maximum adsorption capacity from 434.8 to 476.2 (mg.g⁻¹), suggests endothermic nature of the process. Increasing particle size ranges from 80-128 µm to 500-710 µm led to a decrease in the q_m from 455.0 to 417.4 (mg.g⁻¹). However, increasing solution pH from 2 to 12 led to an increase in q_m from 399.8 to 500.0 (mg.g⁻¹).

Values of R_L for natural MB/clay system have been calculated for all variables studied and found that all values of R_L suggest favorable adsorption process (0<R_L<1). One example allowing an estimation of the R_L value is depicted in Figure 6, which shows plots of R_L against initial MB concentrations at different temperatures. As shown in the Figure all values of R_L lies between (0-1), indicated that the favorability of the adsorption process. The Figure also shows that R_L value decreased with increasing initial MB concentrations suggested that adsorption process was more favorable at higher concentration.

Comparing the maximum adsorption capacity of Bentonite that obtained in this study to that in literature, it was found Yemen Bentonite have very high adsorption capacity compared to that for activated carbon and other adsorbents (Table 3).

3.3.2. Freundlich Isotherm

The experimental equilibrium data for the adsorption of MB onto clay at different temperatures, particle size ranges and solution pH values have been analyzed using the Freundlich isotherm as given by equation 6⁽⁵³⁾.

$$q_e = K_F C_e^{1/n} \quad (6)$$

Where K_F is Freundlich constant (dm³.g⁻¹)ⁿ and n is the heterogeneity factor. The K_F value is related to the adsorption capacity; while 1/n value is related to the adsorption intensity. The magnitude of exponent (n) gives an indication of the favorability and capacity of the adsorbent/adsorbate system. Values of (n) greater than 1 represent favorable adsorption according to Treybal⁽⁵⁴⁾.

Equation 6 may be linearized via a logarithmic plot which enables the exponent (n) and the constant (K_F) to be determined:

$$\log q_e = \log K_F + (1/n) \log C_e \quad (7)$$

The Freundlich parameters (K_F and n) have been calculated using the least-squares method applied to the straight lines that resulted from plotting of $\log q_e$ against $\log C_e$ (not shown) and are listed with the corresponding values of R^2 and ARE in Table 4.

According to the results shown in Table 4, the values of n are greater than unity indicating that the adsorption of MB onto clay is favorable. This is in great agreement with the findings regarding to R_L values.

3.3.3. Temkin Isotherm

The Temkin isotherm has been used in the following form ⁽⁵⁵⁾:

$$q_e = \frac{RT}{b_T} (\ln A_T C_e) \quad (9)$$

Equation (9) can be expressed in its linear form as:

$$q_e = B_T \ln A_T + B_T \ln(C_e) \quad (10)$$

Where

$$B_T = \frac{RT}{b_T} \quad (11)$$

Where T is the absolute temperature (K), R is the universal gas constant ($J.g^{-1}.K^{-1}$), A_T is the equilibrium binding constant corresponding to the maximum binding energy ($dm^3.mg^{-1}$), b_T is Temkin isotherm constant ($J.g^{-1}$) and the constant B_T is related to the heat of adsorption (dimensionless) ⁽¹⁹⁾. According to equation 10, a plot of (q_e) against $\ln(C_e)$ enables the determination of the isotherm constants (A_T and B_T). The values of A_T and B_T are calculated for different variables studied and listed with the corresponding values of R^2 and ARE in Table 4.

3.3.4. Redlich-Peterson Isotherm

The Redlich–Peterson isotherm contains three parameters and involves the features of both the Langmuir and the Freundlich isotherms ⁽⁵⁶⁾. It can be described as follows:

$$q_e = \frac{(K_{RP} \cdot C_e)}{(1 + a_{RP} \cdot C_e^\beta)} \quad (12)$$

Where K_{RP} is the modified Langmuir constant ($dm^3.g^{-1}$), a_{RP} ($dm^3.mg^{-1}$) and β are constant. $\beta \leq 1$.

The linear form is shown in equation (13) from which the constants (K_{RP} , a_{RP} and β) which characterize the isotherm, can be determined:

$$\log\left(\frac{K_{RP}C_e}{q_e} - 1\right) = \log a_{RP} + \beta \log C_e \quad (13)$$

Plotting ($\log [(K_{RP}C_e/q_e) - 1]$) against ($\log C_e$) yields a straight line of slope = β and intercept = $\log a_{RP}$.

The isotherm parameters in equation 12 was calculated using equation 13 are listed with the corresponding values of R^2 and ARE in Table 4.

The results listed in Tables 2 and 4 indicated that Redlich-Peterson isotherm model fit the experimental data for the adsorption of MB onto clay at different temperature, particle size ranges and solution pH values better than the Langmuir, the Freundlich, and the Temkin isotherm based on the very high values of R^2 ($R^2 > 0.999$) and the lower values of ARE compared to other models. The results in Table 2 show that although the very high values of R^2 ($R^2 > 0.999$) for Langmuir model at different variables, the values of ARE for Langmuir are larger than that Redlich-Peterson isotherm. The high values of ARE for Langmuir model can be attributed to the deviation in the experimental data from Langmuir isotherm at low concentrations.

3.4 Thermodynamic Study

The thermodynamic parameters that must be considered to determine the process are changes in Gibbs free energy (ΔG°), standard enthalpy (ΔH°), and standard entropy (ΔS°) due to transfer of unit mole of solute from solution onto the solid-liquid interface.

The Gibbs free energy change of adsorption is defined as:

$$\Delta G^\circ = -2.303 RT \cdot \log K_L \quad (14)$$

Where K_L is Langmuir equilibrium constant ($\text{dm}^3 \cdot \text{g}^{-1}$), (R) is the universal gas constant ($8.314 \text{ J} \cdot \text{g} \cdot \text{mol}^{-1} \cdot \text{K}^{-1}$) and (T) is the absolute temperature (K).

The values of (ΔH°) and (ΔS°) was computed using Van't Hoff equation:

$$\log K_L = \frac{\Delta S^\circ}{2.303R} - \frac{\Delta H^\circ}{2.303RT} \quad (15)$$

A plot of ($\text{Log } K_L$) versus ($1/T$) should produce straight line with slope equals to $-\Delta H^\circ/2.303RT$ and intercept equals to $\Delta S^\circ/2.303R$ ⁽⁵⁷⁾. Figure 7 shows linear relation between ($\text{Log } K_L$) and ($1/T$) with high correlation coefficient ($R^2 > 0.9$). The values of (ΔH°) and (ΔS°) are calculated from the slope and the intercepts of straight line in Figure 7 and listed in Table 5. The values of standard Gibbs free energy (ΔG°) are calculated using equation 14 and also listed in Table 5.

The standard enthalpy (ΔH°) and entropy (ΔS°) changes of adsorption of MB onto clay determined from equation (15) were found to be 32.3 (kJ.g-mol^{-1}) and 152.0 ($\text{J.g-mol}^{-1}.\text{K}^{-1}$) as respectively. The positive value of standard enthalpy (ΔH°) shows that the adsorption is an endothermic process, while the positive value of standard entropy (ΔS°) reflects the increased randomness at the solid/solution interface ⁽⁵⁸⁾.

The values of standard Gibbs energy change (ΔG°) in all the cases are indicative of the spontaneous nature of the interaction without requiring large activation energies of adsorption and no energy input from outside of the system is required. The results in Table 5 show that the negative value of (ΔG°) increase with an increase in temperature, indicating that the spontaneous natures of adsorption of MB were direct proportional to the temperature and higher temperature favored the adsorption imply the greater driving force of adsorption at high temperatures than at low.

4. CONCLUSIONS

This study investigated the equilibrium adsorption of methylene blue onto Yemen bentonite. The maximum adsorption capacity was found to vary with the solution temperature, clay particle size range and solution pH value. Maximum adsorption capacity increased from 435.1 to 476.0 (mg.g^{-1}) with increasing temperature from 15 to 45°C and increased from 417.4 to 455.0 (mg.g^{-1}) with increasing solution pH value from 2 to 12 .However, decreased from 455.0 to 417.4 (mg.g^{-1}) with increasing clay particle size range from 80-125 to 500-710 μm . The Redlich-Peterson isotherm was found to have the best fit to the experimental data over the whole concentration range. The values of thermodynamic parameters ΔG° , ΔH° , and ΔS° indicated that the adsorption process is spontaneous, chemical in nature and favorable at high temperatures. The values of separation factor (R_L) revealed the favorable nature of the adsorption process of the MB/clay system ($0 < R_L < 1$). The study shows that Yemen bentonite can be used as low-cost adsorbent for the removal of methylene blue dye from aqueous solutions.

5. REFERENCES

1. Robinson, T, McMullan, G, Marchant, R, Nigam, P, (2001), "Remediation of dyes in textile effluent: A critical review on current treatment technologies with a proposed alternative" , *Biores. Technol.*, 77 (3), 247-255.
2. Banat, I, M, Nigam, P, Singh, D, Marchant, R, (1996) "Microbial decolorization of textile-dye-containing effluents: A review", *Biores. Technol.* 58, 217-227.
3. Yener, J, Kopac, T, Dogu, G, Dogu, T, (2008), "Dynamic analysis of sorption of methylene blue dye on granular and powdered activated carbon", *Chem. Eng. J.*, 144, 144, 400.
4. Gupta, V, K, Suhas, (2009), "Application of low-cost adsorbents for dye removal: A review", *J. of Environ. Manage.*, 90, 2313–2342.
5. Ghosh, D, Bhattacharyya, K, G, (2002), "Adsorption of methylene blue on kaolinite", *Appl. Clay Sci.* 20, 295– 300.
6. Tsai, W, T, Hsu, H, C, Su, T,Y, Lin, K, Y, Lin, C, M, Dai, T, H, (2007), "The adsorption of cationic dye from aqueous solution onto acid-activated andesite", *J. Hazard. Mater.*, 147, 1056–1062.
7. Jain, A, K, Gupta, V, K, Bhatnagar, A, Suhas, (2003), "Utilization of industrial waste products as adsorbents for the removal of dyes", *J. Hazard. Mater.*, B101, 31–42.
8. Crini, G,(2006), "Non-conventional low-cost adsorbents for dyes removal: A review", *Bioresour. Technol.*, 97, 1061–1085.
9. Chan, L, S, Cheung, W, H, Allen, S, J, McKay, G, (2009), "Separation of acid-dyes mixture by bamboo derived active carbon", *Sep. Purify. Technol.*, 67, 166-172.
10. El-Halwany, M, M, (2010), "Study of adsorption isotherms and kinetic models for methylene blue adsorption on activated carbon developed from Egyptian rice hull", *Desalination*, 250, 208–213.
11. El-Geundi, M, S, (1991), "Colour removal from textile effluents by adsorption techniques", *Water Res.* 25, 271–273.
12. Nassar, M, M, Magdy, Y, H,(1997), "Removal of different basic dyes from aqueous solutions by adsorption on palm-fruit bunch particles", *Chem. Eng. J.*, 66, 223–226.

13. Chen, B, Hui, C, W, McKay, G, (2001), "Pore-surface diffusion modeling for dyes from effluent on pith", *Langmuir*, 17, 740-748.
14. Hameed, B, H, El-Khaiary, M, I,(2008), "Malachite green adsorption by rattan sawdust: Isotherm, kinetic and mechanism modeling", *J. Hazard. Mater.* 159, 574–579.
15. Hameed, B, H, (2009), "Evaluation of papaya seeds as a novel non-conventional low-cost adsorbent for removal of methylene blue", *J. Hazard. Mater.* 162, 939–944.
16. Dögan, M, Abak, H, Alkan, M, (2009), "Adsorption of methylene blue onto hazelnut shell: Kinetics, mechanism and activation parameters", *J. Hazard. Mater.*,164, 172–181
17. Bhattacharyya, K, G, Gupta, S, S, (2008), "Adsorption of a few heavy metals on natural and modified kaolinite and montmorillonite: A review", *Advances in Colloid and Interface Sci.*, 140, 114-131.
18. Rao, P, H, He, M, (2006), "Adsorption of anionic and nonionic surfactant mixtures from synthetic detergents on soils", *Chemosphere*, 63, 1214-1221.
19. Bulut, E, Özacar, M, Şengil, I, A, (2008), "Equilibrium and kinetic data and process design for adsorption of congo red onto bentonite", *J. Hazard. Mater.*, 154, 613-622.
20. Doğan, M, Hamdi, M, Karaoğlu, K, Alkan, M, (2009), "Adsorption kinetics of maxilon yellow 4GL and maxilon red GRL dyes on kaolinite", *J. Hazard. Mater.*, 165, 1142-1151.
21. Barrett, E, P, Joyner, L, G, Halenda, P, P, (1951), "The determination of pore volume and area distributions in porous substances. I. Computations from nitrogen isotherms", *J. Am. Chem. Soc.*, 73, 373-380.
22. Branauer, S, Emmett, P, H, Teller, E, (1983), "Adsorption of gases in multimolecular layers", *J. Am. Chem. Soc.*, 60, 309-315.
23. El-Geundi, M, S, (1990), "Adsorption equilibria of basic dyestuffs onto maize cob", *Adsorption Sci. & Technol.*, 7, 114-123.
24. Gregg, S, J, Sing, K, S, (1982) "Adsorption Surface Area and Porosity", 2nd ed.; London, U.K., Academic Press.
25. Gilles, C, H, Macewan, T, H, Nakhwa, S, N, Smith, D, (1960), "A system of classification of solution adsorption isotherms, and its use in diagnosis of adsorption mechanisms", *J. Chem. Soc.*, 4, 3973–3993.

26. Wang, S, Zhu, Z, H, (2007), "Effects of acidic treatment of activated carbons on dye adsorption", *Dyes Pigm.*, 75, 306–314.
27. Senthilkumaar, P, R, Varadarajan, P, R, Porkodi, K, Subbhuraam, C, V, (2005), "Adsorption of methylene blue onto jute fiber carbon: kinetics and equilibrium studies", *J. Colloid Interface Sci.*, 284, 78–82.
28. Tan, I, A, Ahmad, A, L, Hameed, B, H, (2008), "Adsorption of basic dye using activated carbon prepared from oil palm shell: Batch and fixed bed studies", *Desalination*, 225, 13–28.
29. Han, R, Zhang, J, Han, P, Wang, Y, Zhao, Z, Tang, M, (2009), "Study of equilibrium, kinetic and thermodynamic parameters about Methylene Blue adsorption onto natural zeolite", *Chem. Eng. J.*, 145, 496–504.
30. Al-Degs, Y, Khraisheh, M, A, Allen, J, S, Ahmad, M, N, (2000), "Effect of carbon surface chemistry on the removal of reactive dyes from textile effluent", *Water Res.*, 34, 927-935.
31. Wong, Y, C, Szeto, Y, S, Cheung, W, H, McKay, G, (2008), "Effect of temperature, particle size and percentage deacetylation on the adsorption of acid dyes on chitosan", *Adsorption*, 14,11-20.
32. Ponnusami, V, Vikram, S, Srivastava, S,V, (2008), "Guava (*Psidium guajava*) leaf powder: Novel adsorbent for removal of methylene blue from aqueous solutions", *J. Hazard. Mater.*, 152, 276-286.
33. Özdemir, Y, Doğan, M, Alkan, M, (2006), "Adsorption of cationic dyes from aqueous solutions by sepiolite", *Microporous and Mesoporous Mater.*, 96, 419–427.
34. Kapoor, A. and Yang, R.T. (1989). Correlation of equilibrium adsorption data of condensable vapors on porous adsorbents. *Gas. Sep. Purif.* 3 (4):187–192.
35. Langmuir, I, (1916), "The constitution and fundamental properties of solids and liquids", *J. Am. Chem. Soc.*, 38, 2221-2295.
36. Hall, K, R, Eagleton, L, C, Acrivos, A, Vermeulen, T, (1966), "Pore- and solid-diffusion kinetics in fixed-bed adsorption under constant-pattern conditions", *Ind. Eng. Chem. Fund.*, 5, 212–223.

37. Panday, K, K, Parasad, G, Singh, V, N, (1984), "Removal of Cr (VI) from aqueous solutions by adsorption on fly ash-wollastonite", *J. Chem. Technol. Biotechnol.* 34A, 367-374.
38. Kannan, N, Sundaram, M, M, (2001), "Kinetics and mechanism of removal of methylene blue by adsorption on various carbons—a comparative study", *Dyes Pigments*, 51, 25–40.
39. El Mouzdahir, Y, Elmchaouri, A, Mahboub, R, Gil, A, Korili, S, A, (2010) "Equilibrium modeling for the adsorption of methylene blue from aqueous solutions on activated clay minerals", *Desalination*, 250, 335–338.
40. Okada, K, Yamamoto, N, Kameshima, Y, Yasumori, A, (2003) "Adsorption properties of activated carbon from waste newspaper prepared by chemical and physical activation", *J. Colloid Interface Sci.*, 262, 194–199.
41. Bagane, M, Guiza, S, (2000), "Removal of a dye from textile effluents by adsorption", *Ann. Chim. Sci. Mater.*, 25, 615–626.
42. Almeida, C, A, Debacher, N, A, Downs, A, J, Cottet, L, Mello, C, A, (2009), "Removal of methylene blue from colored effluents by adsorption on montmorillonite clay", *J. Colloid Interface Sci.*, 332, 46–53.
43. Chandra, T, C, Mirna, M, M, Sudaryanto, Y, Ismadji, S, (2007), "Adsorption of basic dye onto activated carbon prepared from durian shell: Studies of adsorption equilibrium and kinetics", *Chem. Eng. J.*, 127, 121–129.
44. Gulnaz, O, Kaya, A, Matyar, F, Arikan, B, (2004), "Sorption of basic dyes from aqueous solution by activated sludge", *J. Hazard. Mater.*, B108, 183–188.
45. Stavropoulos, G, G, A.A. Zabaniotou, A,A, (2005), "Production and characterization of activated carbons from olive-seed waste residue", *Microporous Mesoporous Mater.*, 82, 79–85.
46. Al-Ghouti, M, A, Khraisheh, M, A, Allen, S, J, Ahmad, M, N, (2003), "The removal of dyes from textile wastewater: a study of the physical characteristics and adsorption mechanisms of diatomaceous earth", *J. Environ. Manage.*, 69, 229–238.
47. Dögan, M, Alkan, M, Onager, Y, (2000), "Adsorption of methylene blue from aqueous solution onto perlite", *Water Air Soil Pollut.*, 120, 229–248.

48. Shawabkeh, R, A, Tutunji, M, F, (2003), "Experimental study and modelling of basic dye sorption by diatomaceous clay", *Appl. Clay Sci.*, 24, 111–120.
49. Hong, S, Wen, C, He, J, Gan, F, Ho, Y, S, (2009) "Adsorption thermodynamics of methylene blue onto bentonite", *J. Hazard. Mater.*, 167, 630–633.
50. Özer, D, Dursun, G, Özer, A, (2007), "Methylene Blue adsorption from aqueous solution by dehydrated peanut hull", *J. Hazard. Mater.*, 144, 171–179.
51. Al-Futaisi, A, Jamrah, A, Al-Hanai, R, (2007), "Aspects of cationic dye molecule adsorption to palygorskite", *Desalination*, 214, 327–342.
52. Gurses, A, Karaca, S, Dogar, C, Bayrak, R, Açıkıldız, M, Yalçın, M, (2004), "Determination of adsorptive properties of clay/water system: methylene blue sorption", *J. Colloid Interface Sci.*, 269, 310–314.
53. Freundlich, H, M, (1906), "Over the adsorption in solution", *J. Phys. Chem.*, 57, 385-470.
54. Treybal, R, E, (1985), "Mass transfer operation", 3rd ed.; New York, U.S., McGraw-Hill Book Company.
55. Temkin, M, I, (1941), "Adsorption equilibrium and the kinetics of processes on nonhomogeneous surfaces and in the interaction between adsorbed molecules", *Zh. Fiz. Chim.*, 15, 296-332.
56. Redlich, O, Peterson, D, L, (1959), "A useful adsorption isotherm", *J. Phys. Chem.*, 63, 1024.
57. Cheung, C, W, Porter, J, F, McKay, G, (2001), "Sorption kinetic analysis for the removal of cadmium ions from effluents using bone char", *Water Res.*, 35, 605-612.
58. Smith, J, M, Van Ness, H, C, (1987), "Introduction to Chemical Engineering Thermodynamics", 4ed., Singapore, McGraw-Hill.

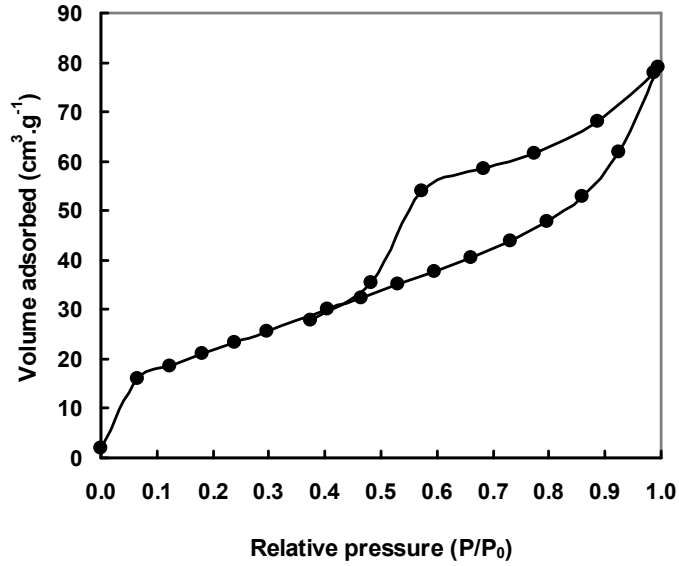


Fig.(1): Adsorption isotherms of bentonite tested with N₂ at 77.35 K.

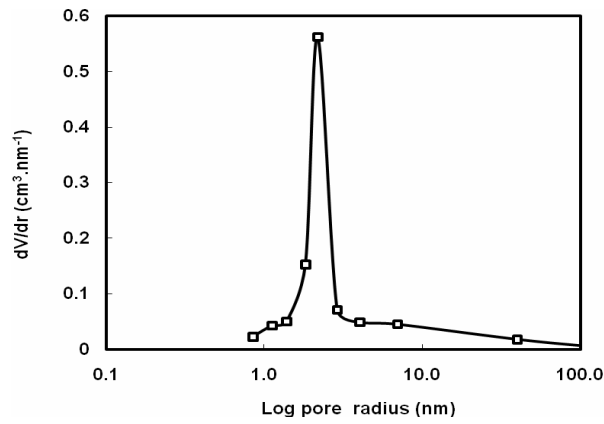


Fig.(2): Pore size distributions of bentonite determined using BJH technique.

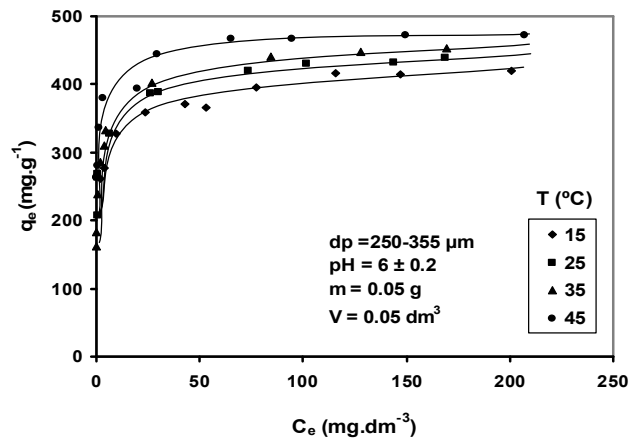


Fig.(3): Adsorption isotherms of MB onto bentonite at different temperatures.

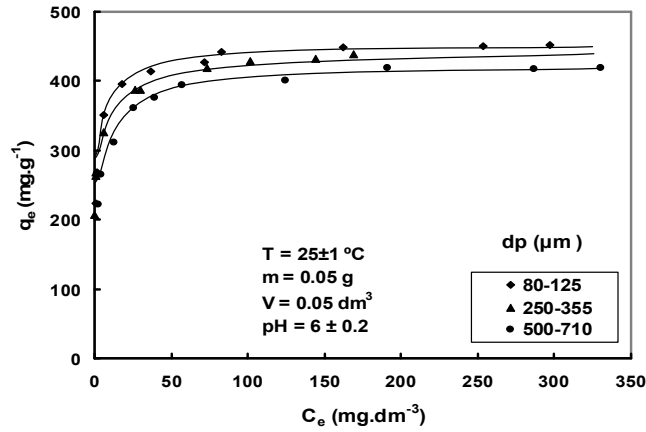


Fig.(4): Adsorption isotherms of MB onto bentonite at different particle size ranges.

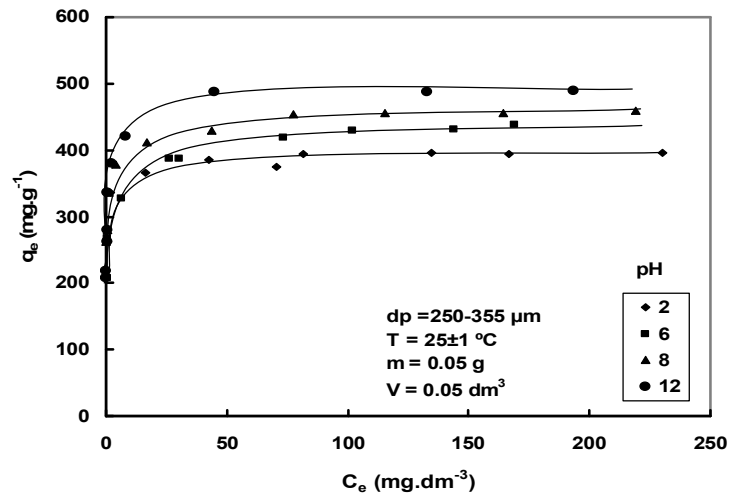


Fig.(5): Adsorption isotherms of MB onto bentonite at different solution pH values.

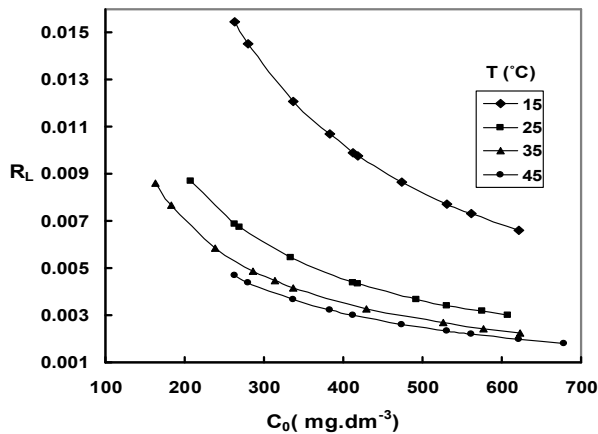


Fig.(6): Plot R_L against initial MB concentration at different temperatures.

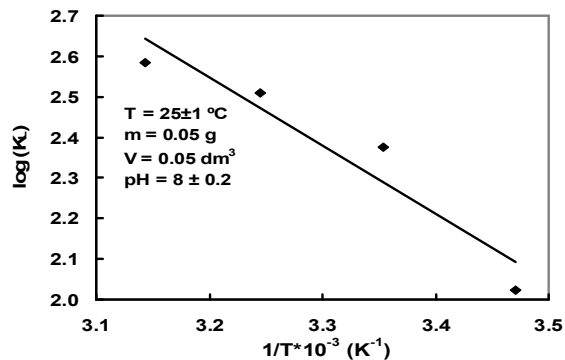


Fig.(7): Plot of Log K_L against $1/T$ for the adsorption of MB onto bentonite.

Table (1): Surface characteristics of bentonite.

Total surface area (S_{BET}) ($m^2 \cdot g^{-1}$)	82.34
Total pore volume (V_T) ($cm^3 \cdot g^{-1}$)	0.109
Average pore radius (r_{av}) (Å)	26.40
Micropore volume (V_{mic}) ($cm^3 \cdot g^{-1}$)	0.012
Mesopore volume (V_{mes}) ($cm^3 \cdot g^{-1}$)	0.096
Macropore volume (V_{mac}) ($cm^3 \cdot g^{-1}$)	0.001
Solid-phase density (ρ_s) ($g \cdot cm^{-3}$)	2.526
Particle density (ρ_p) ($g \cdot cm^{-3}$)	1.859
Particle porosity (ϵ_p)	0.264

Table (2): Estimated Langmuir model and Freundlich model parameters for the adsorption of MB onto bentonite at different variables.

Parameter	Langmuir					Freundlich			
	K_L	a_L	q_m ($mg \cdot g^{-1}$)	R^2	ARE	K_F	n	R^2	ARE
T(°C)									
15	105.3	0.242	435.1	0.9998	0.1131	249.7	9.67	0.8994	0.0224
25	238.1	0.548	434.5	0.9995	0.2054	265.2	9.55	0.9555	0.0402
35	322.6	0.710	454.4	0.9997	0.1894	235.9	6.90	0.937	0.0803
45	384.6	0.808	476.0	0.9998	0.1735	296.4	10.00	0.9404	0.0460
dp μm									
80-125	196.1	0.431	455.0	0.9999	0.1002	261.5	9.07	0.9041	0.0613
250-355	238.1	0.548	434.5	0.9995	0.2054	265.2	9.55	0.9555	0.0402
500-710	101.0	0.242	417.4	0.9998	0.0540	221.4	8.14	0.8994	0.0452
pH									
2	384.6	0.962	399.8	0.9998	0.1138	293.0	15.95	0.868	0.0420
6	238.1	0.548	434.5	0.9995	0.2054	265.2	9.55	0.9555	0.0402
8	434.8	0.957	454.3	0.9999	0.1686	312.1	12.03	0.9351	0.0431
12	1000.0	2.000	500.0	1.0000	0.1394	289.1	8.67	0.8722	0.0975

Table (3): Adsorption capacity (q_m) of methylene blue on to various adsorbents.

Adsorbent	q_m (mg.g^{-1})	Sources
Commercial activated carbon	980.3	(38)
Activated clay (Moroccan)	558.0	(39)
Yemen bentonite	500.0	The present work
Straw activated carbon	472.1	(38)
Coconut husk-based activated carbon	434.8	(29)
Activated carbon prepared from waste newspaper	390.0	(40)
Clay (Tunisia)	300.0	(41)
Montmorillonite clay	289.1	(42)
Activated carbon prepared from durian shell	289.3	(43)
Activated sludge biomass	256.4	(44)
Activated carbon prepared from oil palm shell	243.9	(29)
Filtrisorb F300a	240.0	(45)
Diatomite (Jordan)	198.0	(46)
Perlite	162.3	(47)
Diatomite (Jordan)	156.6	(48)
Bentonite	150.0	(49)
Bamboo dust-based activated carbon	143.2	(38)
Dehydrated peanut hull	123.5	(50)
Palygroskrite	50.8	(51)
Clay (Turkey)	6.3	(52)

Table (4): Estimated Temkin model parameters and Redlich-Peterson model parameters for the adsorption of MB onto bentonite at different variables.

Parameter	Temkin				Redlich-Peterson				
	B_T	A_T	R^2	ARE	K_{RP}	a_{RP}	β	R^2	ARE
T(°C)									
15	34.93	980.3	0.9350	0.0183	1712.8	6.365	0.9130	0.9986	0.0177
25	33.87	2891.0	0.9817	0.0302	1800.0	5.200	0.9581	0.9995	0.0275
35	43.62	289.7	0.9854	0.0380	1905.3	6.368	0.9154	0.9999	0.0172
45	32.44	17222.6	0.9588	0.0376	1935.4	4.588	0.9837	0.9990	0.0371
dp μm									
80-125	37.41	1110.1	0.9430	0.0458	2010.5	6.920	0.9120	0.9993	0.0399
250-355	33.87	2891.0	0.9817	0.0302	1800.0	5.200	0.9581	0.9995	0.0275
500-710	39.87	186.8	0.9350	0.0406	940.7	3.904	0.8942	0.9986	0.0411
pH									
2	23.67	134787.3	0.9827	0.1379	1613.8	4.475	0.9828	0.9996	0.0246
6	33.87	2891.0	0.9817	0.0302	1800.0	5.200	0.9581	0.9995	0.0275
8	28.99	59610.2	0.9661	0.0326	2100.5	4.917	0.9914	0.9993	0.0291
12	40.13	2316.9	0.9287	0.0792	2100.5	4.917	0.9914	0.9995	0.0301

Table (5): Thermodynamic parameters for the adsorption of MB onto bentonite.

T (K)	ΔG° (kJ.g-mol ⁻¹)	ΔH° (kJ.g-mol ⁻¹)	ΔS° (J.g-mol ⁻¹ .K ⁻¹)	R ²
288.15	-11.2	+32.3	+152.0	0.906
298.15	-13.6			
308.15	-14.8			
318.15	-15.7			

إزالة أزرق الميثيلين من المحاليل المائية باستخدام البنتونايت اليمني

هاني احمد قاسم دماج

عبد الرقيب عبد الوهاب مسعد الوهبي

أستاذ مشارك

أستاذ مشارك

قسم الهندسة الكيميائية - كلية الهندسة والبتترول - جامعة حضرموت للعلوم والتكنولوجيا -

المكلا- حضرموت- اليمن

الخلاصة

في هذه الدراسة تم دراسة إزالة أزرق الميثيلين من المحاليل المائية باستخدام طفلة البنتونايت اليمنية كدالة في درجة الحرارة المحلول وحجم جزيئات البنتونايت والرقم الهيدروجيني للمحلول. أوضحت النتائج أن سعة إمتزاز أزرق الميثيلين تزداد بزيادة درجة حرارة المحلول وزيادة الرقم الهيدروجيني للمحلول ونقصان حجم الجزيئات. وقد وجد أن أقصى سعة إمتزاز هي ٥٠٠ ملجم صبغة لكل جرام من البنتونايت عند درجة حرارة ٢٥ درجة مئوية ورقم هيدروجيني ١٢ وحجم جزيئات (٢٥٠-٣٥٥ ميكرون). تم تحليل النتائج باستخدام أربعة نماذج إتزان هي نموذج لانجمير وفرندليش وتمكين وردليك - بترسون وقد وجد أن نموذج ردليك - بترسون يعطي أفضل تمثيل للنتائج. تم إيجاد المتغيرات الديناميكية الحرارية مثل طاقة جيبس الحرة القياسية والإنتالبي القياسية والإنتروبي القياسية وإشارة قيم هذه المتغيرات إلى أن عملية إمتزاز أزرق الميثيلين بواسطة البنتونايت هي عملية لحضية وماصة للحرارة. بينت النتائج أن البنتونايت اليمني ذو فعالية عالية في إزالة أزرق الميثيلين من المحاليل المائية ورخيص التكلفة ويمكن استخدامه كبديل للمواد ألمازة العالية التكلفة.